

Laser Induced Periodic Surface Structures on 100Cr6 Steel for Modification of Friction Demonstrated with Stribeck Test

Stefan Rung¹, Kevin Bokan¹, Kevin Rutsch¹, Simon Schwarz¹, Cemal Esen² and Ralf Hellmann¹

¹ Applied Laser and Photonics Group, University of Applied Sciences Aschaffenburg, Wuerzburger Strasse 45, 63743 Aschaffenburg, Germany

E-mail: Stefan.rung@h-ab.de

² Applied Laser Technologies, Ruhr-University Bochum, Universitaetsstrasse 150, Bochum 44801, Germany

In this contribution, we report on surface functionalization by introducing laser induced periodic surface structures on 100Cr6 bearing steel to modify complex tribological properties. The advanced approach of this study is the measurement of the coefficient of friction by performing a ball-on-disk Stribeck test on laser structured surfaces with polytetrafluoroethylene balls in a lubricant environment. The Stribeck test reveals the modified friction behavior using translation speeds up to 10⁶ mm/min and load forces between 100 mN and 5000 mN. Our results show increased stiction and coefficient of friction for laser structured surfaces in the regime of boundary lubrication which is attributed to the laser induced surface asperities. Decreased coefficient of friction is observed in the regime of mixed and hydrodynamic lubrication, i.e. for velocities higher than 1000 mm/min, for surfaces covered by laser induced periodic surface structures with low spatial frequency.

DOI: 10.2961/jlmn.2018.03.0004

Keywords: laser-induced periodic surface structures; tribology; Stribeck test

1. Introduction

Power generation, production engineering and transportation of goods are, from a very fundamental point of view, based on machines which involve a variety of moving parts and interacting surfaces. Ecological and economical aspects, such as energy efficiency, long-term stability and reliability are effectively determined by the friction and wear between interacting surfaces. A recent study reveals that about 23% of the world's energy consumption and 8120 Mt/year of CO₂ emission are caused by these tribological effects, in turn posing the necessity for wear and friction control [1]. While laser based surface functionalization has already been intensively studied during the last decade, femtosecond laser technology has recently expedited surface structuring on different length scales to advance tribological properties [2–5]. In particular, the formation of Laser Induced Periodic Surface Structures (LIPSS) has been investigated on different materials like metals [6; 7], dielectrics [8; 9] and semiconductors [10; 11]. These fs-laser induced surface morphologies can be generated in a single-step process and provide multiple possibilities to modify different surfaces properties. Possible applications involve colorization due to diffraction at the periodic structures [12; 13], modification of surface wetting properties [14; 15], influence on surface cell growth [16; 17] and friction management [18; 19]. Generally, LIPSS are categorized into 3 groups, namely low spatial frequency LIPSS (LSFL), high spatial frequency LIPSS (HSFL) and cone like protrusions (CLP).

In this study, we use LSFL to alter tribological properties. These structures appear upon laser irradiation with linear polarized light. The origin of LSFL is commonly explained by an interference effect of the incident laser light and a surface electro-magnetic wave generated by a laser induced surface plasmon polariton (SPP). Due to this origin, LSFL occur

with a spatial periodicity in the range of the used laser wavelength and an orientation perpendicular to the polarization of the laser light. Several research groups have shown that LSFL properties like spatial period, orientation and homogeneity can be also controlled by the applied laser fluence [20; 21], pulse to pulse overlap [22] and initial surface roughness of the solid material [23].

While, in general, friction properties of surfaces depend next to the specific materials considered on several properties of the sliding surface itself, the properties of the counter body, the sliding speed, the environmental conditions and the nature of any lubricant, it is obvious that numerous experimental studies are needed to get fully acquainted with the effects of laser induced periodic surface structures on such tribological properties.

From a very general point of view, lubricated friction as investigated here can be categorized into boundary, mixed and hydrodynamic regimes. At the beginning of the relative motion between sliding partners and at low speeds, friction is governed by their physical contact. This may also occur during heavy load conditions. In this regime, the lubrication solvent thickness is smaller than the surface roughness. For bearing and journal materials, e.g., this is the most undesirable regime as it is characterized by a high coefficient of friction (i.e. energy loss) and increased wear.

With increasing sliding speed a wedge or slice of lubricant is created between the surfaces and boundary lubrication is significantly reduced. As the lubricant film thickness increases and asperity contact is reduced, friction decreases leading to a state denoted as mixed lubricant regime. Mixed refers to a state that can be described by an increasing lubricant film thickness and by remaining asperities between the sliding partners being loaded with lubricant. With continuously increasing sliding speed, this condition is translated to

$$F(u, v) = \sum_{x=0}^{X-1} \sum_{y=0}^{Y-1} f(x, y) * e^{-i2\pi\frac{xu}{X}} * e^{-i2\pi\frac{yv}{Y}} \quad (1)$$

Herein u and v are spatial frequencies in x and y directions, whereas $F(u, v)$ is the two-dimensional spectrum of the microscope image $f(x, y)$. X and Y represent the size of the image $f(x, y)$.

The disk for the Stribeck test is a round 100Cr6 steel disk with a diameter of 70 mm and a thickness of 6.6 mm. Before the laser modification is carried out, the base plate was prepared by grinding and polishing with a multi directional polishing with several abrasive strength and afterwards polished with suspensions down to a grain size of 1 μm to achieve a reference surface with a roughness R_a of 14 nm. To investigate the influence of laser induced periodic surface structures on the COF, concentric rings, filled with LIPSS were produced on the steel surface (c.f. Fig. 1 b and c).

The measurement of the COF was performed in a ball-on-disk setup. We used the Universal Mechanical Tester from Bruker (UMT TriboLab) to perform the Stribeck test. The system is equipped with a rotation drive allowing rotation speeds up to 5000 rpm and a second drive unit to apply a specific load of the ball on the base plate. The used force sensor allows measuring the load F_L and the lateral force F_X up to 5 N. The resulting COF is calculated by F_X / F_L . We measured the friction behaviour of commercially available polytetrafluoroethylene (PTFE, Teflon) in a ball shape with a diameter of 6.3 mm. The ball holder and the force sensor are fixed on a moveable stage along the radius of the disk. Thus either structured surfaces or reference surfaces in different tracks on concentric rings can be measured. During the complete Stribeck Test the rotation disk is covered with engine oil (5W40). A special liquid chamber allows a steady presence of lubricant between the disk and the ball

Due to the elastic deformation of the Teflon ball, different contact areas appear. Using a Hertzian deformation model of a sphere in contact with a flat sample, the diameter of the contact area is calculated to 151 μm , 328 μm and 562 μm for 100 mN, 1000 mN and 5000 mN, respectively.

3. Results and discussion

3.1 LSFL generation

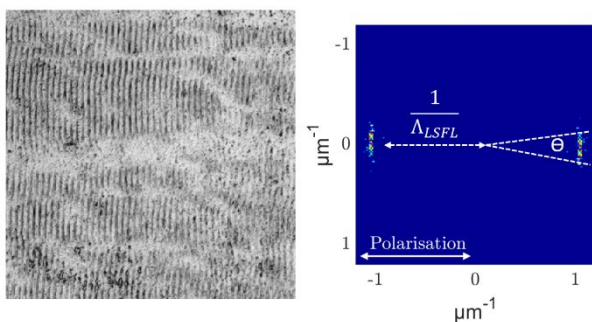


Fig. 3 Microscope image of LSFL (left) and corresponding transformed 2D FFT spectra (right) for the analysis of LSFL generated using 0.29 J/cm² and 80% overlap.

In the first step, the required laser parameters for continuous planar LSFL generation on 100Cr6 steel are

determined with the laser fluence being varied between 0.15 J/cm² and 0.65 J/cm². The pulse overlap is investigated in a range of 70% to 90%, resulting in a spatial pulse to pulse distance of 10.8 μm to 3.6 μm with the scanning speed between 3250 mm/s and 1080 mm/s. Please note that for a homogenous energy deposition, the given pulse overlap holds for both, the consecutive laser pulses inside a scanning track and the overlap of the individual scanning tracks, i.e. the spatial distance between the deposited pulses equals the hatch pitch of the structured surface area.

To produce regular LSFL on the surface, the scanning direction is set orthogonal to the polarization of the laser light. Due to this method, the connection quality of LSFL between the individual scanning tracks is improved [7]. The influence of the laser fluence and the pulse to pulse overlap on the LSFL generation is evaluated by 2D FFT. A microscope image of LSFL covered surfaces and the corresponding 2D FFT spectra are shown in Fig. 3. Less pronounced LSFL with inferior homogeneity and quality are generated using a pulse overlap of 80% and a laser fluence of 0.29 J/cm². In the 2D FFT spectra this evidences in a recognizable opening angle Θ , which in turn can be considered as a quality measure for uniform LSFL. The distance between the center of the 2D FFT and the peak of the frequency sickle represents the mean of the spatial period of the generated LSFL.

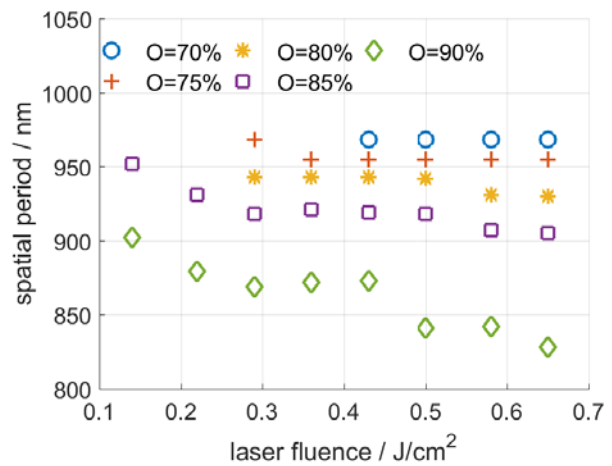


Fig. 4 Spatial period of LSFL for different pulse overlap values as a function of the laser fluence.

All investigated processing parameters lead to a complete LSFL coverage on the 100Cr6 steel surface. The general morphology is similar to the structures shown in Fig 3 and Fig 6. Rung et al. [14] determined a $|\sin(x)|$ - like surface profile description of LSFL on brass using an AFM measurement. Fig 4 shows the resulting spatial periods of LSFL on stainless steel. The inverse value of the 2D FFT centroid is plotted against the laser fluence for pulse overlap values of 70%, 75%, 80%, 85% and 90%, respectively. With decreasing overlap, the required laser fluence increases to generate fully covered LSFL surfaces. With increasing laser fluence and increasing pulse overlap, the spatial period of LSFL decreases. This behavior can be explained by the generation of a surface plasma wave through the parametric decay of laser light [21] and a feedback mechanism based on a

grating assisted SSP excitation and the incident laser radiation [22].

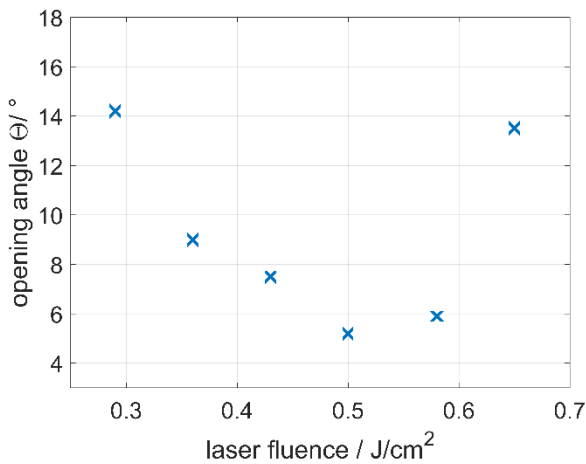


Fig. 5 Opening angle of FFT sickle as a function of the laser fluence for a pulse overlap of 80%

The resulting opening angle of the 2D FFT sickle is shown in Fig. 5 for a pulse overlap of 80%. A laser fluence of 0.29 J/cm² leads to an incomplete LSFL surface covering which results in a large spread angle. With increasing laser fluence the uniformity of the LSFL increases, i.e. Θ decreases. The smallest spread angle can be achieved using a laser fluence of 0.5 J/cm². For a yet further increased fluence surface damage and burr formation is observed, deteriorating LSFL quality and uniformity.

3.2 Tribological evaluation by Stribeck test

As a result of section 3.1., continuous planar LSFL with high homogeneity are generated for the tribological tests using a laser fluence of 0.5 J/cm² and a pulse overlap of 80% (cf. Fig. 6). This parameter set results in LSFL having a period of 942nm (see Fig. 4). In comparison to this periodicity, the calculated contact area of the PTFE counter body (up to a diameter of 562 μ m for 5 N) is much larger, excluding a direction depended friction behavior to be observable in our test. Three concentric rings with a width of 5 mm are filled with LSLF (c.f. orange rings in Fig. 1 b) with the unstructured, polished areas between these rings being used as the reference surface for the tribological test.

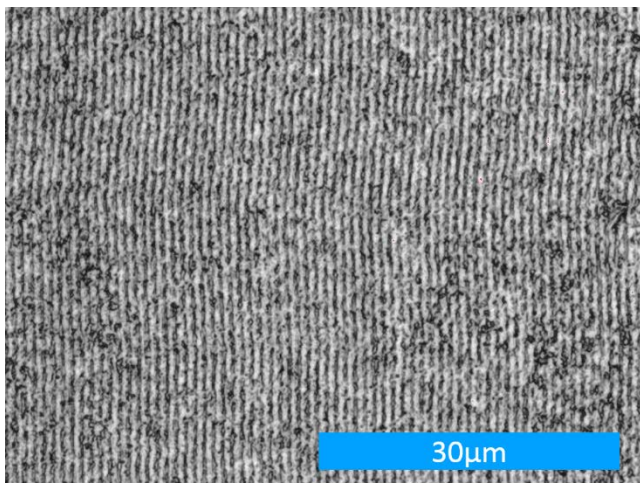


Fig. 6 Microscope image of LSFL on 100Cr6 steel using 0.5 J/cm² and 80% pulse overlap.

The Stribeck test is performed by subsequently increasing the rotation speed. The used steps are (1, 2, 5, 10, 20, 50, 100, 500, 1000, 2000, 3000, 4000, 5000) rpm. Each of this steps is performed for 60 s using a data acquisition rate of 100 Hz, allowing collection of sufficient data for an accurate result. For each load force (100 mN, 1000 mN and 5000 mN), a structured disc is prepared. By the application of three LSFL covered test tracks, the load specific Stribeck tests are performed three times with identical testing conditions for LSFL and reference surface, respectively. All following graphs are the result of the combination of this three-fold measurement approach. The mean value and the standard deviation for each rotation speed step is calculated. By the combination of rotation speed and track radius the specific translation speed is calculated and plotted in the following Stribeck curves. For all evaluated normal loads, no wear on the disc surface, neither on the structured nor on the reference surface can be observed.

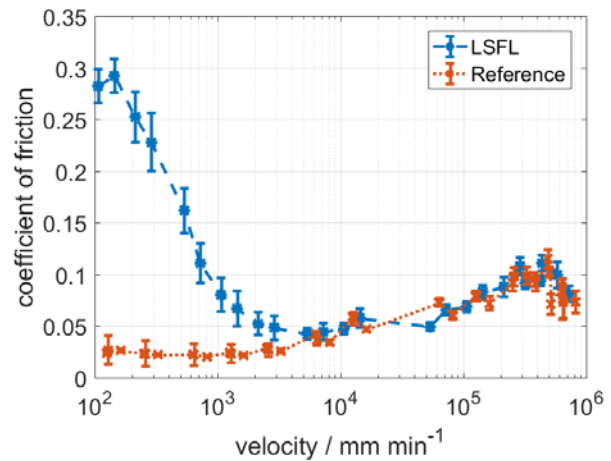


Fig. 7 Stribeck curve for LSFL covered surface (blue) and reference (orange) using a normal load of 100 mN.

Fig. 7 depicts the Stribeck curve for an applied normal load of 100 mN. The orange curve shows the coefficient of friction against the sliding velocity on the polished reference surface. Even for the slowest sliding velocity, the COF is very small, i.e. no distinctive stiction occurs, which is a typical behavior for Teflon on a smooth steel surface [33]. With increasing sliding speed, the COF increases to values of approx. 0.1 indicating the transition to full film hydrodynamic lubrication. The blue curve in Fig. 7 represents the friction behavior of the LSFL covered surface. Contrary to the reference surface, a pronounced stiction is caused by the laser nanostructures, i.e. increased boundary layer lubrication. The COF is increased by a factor of approx. 10 for the slowest sliding speed around 10² mm/min. With increasing velocity, the COF decreases and reaches a local minimum at 0.04 for 5300 mm/min, almost coincident with the COF of the reference. As outlined in the introduction, this general characteristic of lubricant friction can be attributed to the increasing lubricant film thickness between the two sliding partners. With further increasing velocity, the Stribeck curve of the LSFL structured surface is almost identical to the one of the reference surface. Apparently, for a normal load of 100 mN, the nanostructures do not influence the COF in this

hydrodynamic regime by a dominating full film lubrication. Thus, the lubricant film thickness appears to be sufficiently larger than the modulation depth of the LSFL and the lubricated contact does not suffer from a temporal short lubricant supply, i.e. no starvation effects hindering the lubricant to fill the contact inlets between the substrate and the tribometer ball adequately [34].

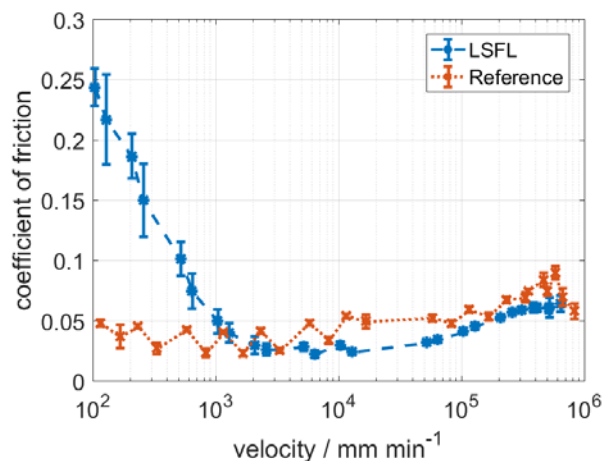


Fig. 8 Stribeck curve for LSFL covered surface (blue) and reference (orange) using a normal load of 1000 mN.

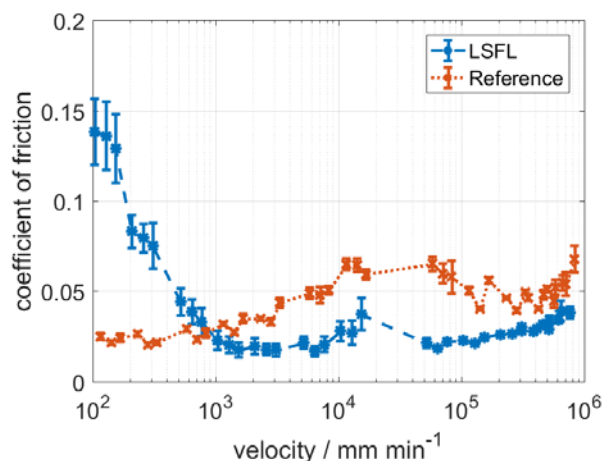


Fig. 9 Stribeck curve for LSFL covered surface (blue) and reference (orange) using a normal load of 5000 mN.

The Stribeck curves for an increased normal load of 1000 mN are shown in Fig. 8, revealing an almost similar behavior of a stronger stiction of LSFL covered surfaces for low velocities (by a factor of 5) and decreasing COF with increasing velocity, accomplishing the COF of the unstructured, polished reference surface in the range between 1000 to about 3000 mm/min. For higher velocities, however, friction on the reference surface exceeds the COF of the LSFL covered specimen for sliding speeds above 10000 mm/min. This indicates that under this higher load full film lubrication is not yet fully formed for the LSFL structured surfaces for these sliding speeds as the generated nanostructures may impede undisturbed engine oil film lubrication.

With a further increase of the normal load to 5000 mN, we find an even more pronounced effect of the LSFL structuring on the COF, as shown in Fig. 9. Again, for lower velocities the COF is increased by a factor of 5 for the laser

nanostructured surface as compared to the reference polished surface. However, with increasing velocity the COF for the LSFL structured specimen equals the one of the reference surface, again by trend as compared to the results shown in Fig. 7 and Fig. 8, for lower speeds already in the range of below 1000 mm/s, with the COF continuously being lower for the LSFL structured surfaces. Again, this indicates changes in the governing mixed lubricant and hydrodynamic regime, namely a shift of the transition from the mixed to the hydrodynamic regime to higher velocities with increasing load for LSFL structured surfaces.

4. Conclusion

We report on tribological surface functionalization upon laser induced periodic surface structures on 100Cr6 steel. In combination with PTFE, a ball on disk setup is used to perform a Stribeck test in an engine oil environment. LSFL covered surfaces lead to a PTFE untypical stiction increase. For a test load of 100 mN, a 10-fold increase of the stiction is caused by LSFL. From an application point of view, this effect is beneficial for all kinds of force and torque transmission. With increasing sliding speed, the coefficient of friction decreases. The slope of this curve increases with increasing test load. Using 5000 mN load, it is possible to reduce lubricated sliding friction for velocities between 10^3 mm/min and 10^6 mm/min. In this regime, the LSFL covered surfaces could lead to a decreased energy loss for moving parts and also a decreased wear generation.

Acknowledgment

This work has been supported within the BMBF project LAMILE (grant 03FH030IX4).

References

- [1] K. Holmberg and A. Erdemir: *Friction*, 5, (2017), 263.
- [2] A. Ancona, G. Carbone, M. de Filippis, A. Volpe and P. M. Lugarà: *Adv. Opt. Technol.*, 3, (2014), 42.
- [3] F. P. Mezzapesa, M. Scaraggi, G. Carbone, D. Sorgente, A. Ancona and P. M. Lugarà: *Physics Procedia*, 41, (2013), 677.
- [4] M. Scaraggi, F. P. Mezzapesa, G. Carbone, A. Ancona, D. Sorgente and P. M. Lugarà: *Tribol. Int.*, 75, (2014), 123.
- [5] A. Ancona, G. Joshi, A. Volpe, M. Scaraggi, P. Lugarà and G. Carbone: *Lubricants*, 5, (2017), 41.
- [6] B. K. Nayak and M. C. Gupta: *Opt. Lasers Eng.*, 48, (2010), 940.
- [7] I. Gnilitzkyi, T. J.-Y. Derrien, Y. Levy, N. M. Bulgakova, T. Mocek and L. Orazi: *Sci. Rep.*, 7, (2017), 8485.
- [8] S. Schwarz, S. Rung and R. Hellmann: *Appl. Phys. Lett.*, 108, (2016), 181607.
- [9] J. Bonse, J. Krüger, S. Höhm and A. Rosenfeld: *J. Laser Appl.*, 24, (2012), 42006.
- [10] T. J.-Y. Derrien, J. Krüger, T. E. Itina, S. Höhm, A. Rosenfeld and J. Bonse: *Appl. Phys. A*, 117, (2014), 77.
- [11] M. Birnbaum: *J. Appl. Phys.*, 36, (1965), 3688.
- [12] A. Y. Vorobyev and C. Guo: *Laser Photonics Rev.*, 7, (2013), 385.
- [13] G. Li, J. Li, Y. Hu, C. Zhang, X. Li, J. Chu and W. Huang: *Appl. Phys. A*, 118, (2015), 1189.

(Received: June 24, 2018, Accepted: October 7, 2018)

- [14] S. Rung, S. Schwarz, B. Götzendorfer, C. Esen and R. Hellmann: *Appl. Sci.*, 8, (2018), 700.
- [15] D. van Ta, A. Dunn, T. J. Wasley, J. Li, R. W. Kay, J. Stringer, P. J. Smith, E. Esenturk, C. Connaughton and J. D. Shephard: *Appl. Surf. Sci.*, 371, (2016), 583.
- [16] O. Raimbault, S. Benayoun, K. Anselme, C. Mauclair, T. Bourgade, A.-M. Kietzig, P.-L. Girard-Lauriault, S. Valette and C. Donnet: *Mater. Sci. Eng. C Mater. Biol. Appl.*, 69, (2016), 311.
- [17] K. Wallat, D. Dörr, R. Le Harzic, F. Stracke, D. Sauer, M. Neumeier, A. Kovtun, H. Zimmermann and M. Epple: *J. Laser Appl.*, 24, (2012), 42016.
- [18] C. Gachot, A. Rosenkranz, L. Reinert, E. Ramos-Moore, N. Souza, M. H. Müser and F. Mücklich: *Tribol Lett.*, 49, (2013), 193.
- [19] A. Ancona, G. Carbone, M. Scaraggi, F. P. Mezzapesa, D. Sorgente and P. M. Lugarà: *SPIE LASE. San Francisco, California, United States, SPIE Proceedings* (2014, 896806.
- [20] E. V. Golosov, V. I. Emel'yanov, A. A. Ionin, Y. R. Kolobov, S. I. Kudryashov, A. E. Ligachev, Y. N. Novoselov, L. V. Seleznev and D. V. Sinitsyn: *Jetp Lett.*, 90, (2009), 107.
- [21] K. Okamuro, M. Hashida, Y. Miyasaka, Y. Ikuta, S. Tokita and S. Sakabe: *Phys. Rev. B*, 82, (2010), 1.
- [22] J. Bonse and J. Krüger: *J. Appl. Phys.*, 108, (2010), 34903.
- [23] F. Preusch, S. Rung and R. Hellmann: *J. Laser. Micro/Nanoengin.*, 11, (2016), 137.
- [24] R. Stribeck: *Z. Verein. Deut. Ing.*, 46, (1902), 38.
- [25] J. Bonse, R. Koter, M. Hartelt, D. Spaltmann, S. Pentzien, S. Höhm, A. Rosenfeld and J. Krüger: *Appl. Phys. A*, 117, (2014), 103.
- [26] J. Eichstädt, G. Römer and A. H. i. Veld: *Physics Procedia*, 12, (2011), 7.
- [27] J. Bonse, S. V. Kirner, M. Griepentrog, D. Spaltmann and J. Krüger: *Materials (Basel)*, 11, (2018).
- [28] Z. Wang, Q. Zhao and C. Wang: *Micromachines*, 6, (2015), 1606.
- [29] D. Braun, C. Greiner, J. Schneider and P. Gumbsch: *Tribol. Int.*, 77, (2014), 142.
- [30] A. Kovalchenko, O. Ajayi, A. Erdemir, G. Fenske and I. Etsion: *Tribol. Int.*, 38, (2005), 219.
- [31] J. W. Robinson, Y. Zhou, P. Bhattacharya, R. Erck, J. Qu, J. T. Bays and L. Cosimbescu: *Sci. Rep.*, 6, (2016), 18624.
- [32] A. Martini, D. Zhu and Q. Wang: *Tribol Lett.*, 28, (2007), 139.
- [33] P. M. Dickens, J. L. Sullivan and J. K. Lancaster: *Wear*, 112, (1986), 273.
- [34] R. Kumar, P. Kumar and M. Gupta: *International Journal of Advancements in Technology*, 1, (2010), 73.

(Received: June 24, 2018, Accepted: October 7, 2018)